Journal of Power and Energy Engineering, 2025, 13(8), 192-205
https://www.scirp.org/journal/jpee
ISSN Online: 2327-5901
ISSN Print: 2327-588X

LES Simulation of the Loop-Shaped Stator Core Duct of an Air-Cooled Turbogenerator

Dmitry Verkhovtsev[1], Anton Permut[1], Maksim Maiantcev[1], Sergey Chishko[2]

[1]Field Tests Department, JSC "Power Machines", Saint Petersburg, Russia
[2]Higher School of Electric Power Systems, Institute of Energy, Peter the Great St. Petersburg Polytechnic University, Saint Petersburg, Russia
Email: dm.verkhovtsev@gmail.com

How to cite this paper: Verkhovtsev, D., Permut, A., Maiantcev, M. and Chishko, S. (2025) LES Simulation of the Loop-Shaped Stator Core Duct of an Air-Cooled Turbogenerator. *Journal of Power and Energy Engineering*, **13**, 192-205.
https://doi.org/10.4236/jpee.2025.138011

Received: July 5, 2025
Accepted: August 23, 2025
Published: August 26, 2025

Abstract

The development of an algorithm for numerical simulation of the loop-shaped stator core duct of the air-cooled turbogenerator has been undertaken for the purpose of studying the character of air flow in it, finding the places of recirculation and determining the aerodynamic characteristics. In the numerical algorithm, two methodologies for modelling turbulent flows are considered: firstly, stationary methods, namely RANS (Reynolds-averaged Navier-Stokes equations) using the Menter's Shear Stress Transfer (SST) turbulence model; and secondly, non-stationary methods, namely large eddy simulation (LES) using the dynamic subgrid-scale Smagorinsky model (DSG). A comparison of these calculation methods with experimental results has been carried out. It is evident that, upon the attainment of the aerodynamic characteristics of the duct and the measurement of the pressure drop across the air coolers during the unit operation, the determination of the actual air flow rate through the stator core of the main packages will be possible. The present study demonstrates that the aerodynamic characteristics obtained by the LES and RANS methods yield close results in the area of the expected design air flow rate of 3.25 l/s at a rated speed 3000 rpm of the turbogenerator. The discrepancy between these results and the experimental value does not exceed 8%. Concurrently, the LES method offers a realistic depiction of the temporal progression of airflow, thereby enabling estimations of the vortices' structure and pressure fluctuations. Conversely, RANS does not necessitate a protracted computation time and facilitates the acquisition of an averaged depiction of the flow with a satisfactory degree of accuracy. Moreover, it does not demand labour-intensive tuning of the solver to ensure the convergence of the problem. The validation of the computational algorithm was carried out on a full-scale experimental model of the duct. The experimental model was created using additive technologies, namely, it was created on a 3D printer from PLA plastic and de-

scribes the duct geometry and surface roughness with high accuracy.

Keywords

Electrical Machine, Turbogenerator Cooling System, Loop-Shaped Stator Core Duct, Aerodynamics, LES and RANS Simulations, SST Model, DSG Subgrid, Additive Technologies

1. Introduction

The enhancement of the active power of air-cooled turbogenerators is inextricably linked to the continual refinement of cooling systems.

The implementation of a comprehensive air-cooling system for large-capacity turbogenerators represents a novel engineering paradigm. In the co-modern stage, the following factors are given consideration: the optimal choice of winding scheme and number of parallel branches [1], the use of a new anisotropic phenomenological model of iron losses taking into account material properties [2]-[3], the use of insulating materials with increased thermal conductivity [4], and, of great importance, the selection and intensification of the cooling system [5]-[8]. This phenomenon can be attributed to the advancements in air-cooled turbo generators, which have attained substantial power ratings. For instance, Gen A (GE) has achieved up to 400 MVA [9] and SGen-1000A (Siemens) has attained up to 370 MVA [10].

The relevance of intensification of the cooling system of air-cooled turbogenerators remains constant, and is contingent on the ongoing development of modern numerical methods for calculating aerodynamics problems [8] [11] [12]. In this context, the library of turbulence models is expanding, with methods for solving stationary and non-stationary problems, and their models for the energy industry, being adapted. Furthermore, optimisation problems are being performed [13], and there is a wide introduction of validation of computational models by means of full-scale experimental models based on additive technologies.

In the turbogenerator of the T3F series of the Elektrosila plant, a physical separation of the stator and rotor cooling circuits has been performed. This has resulted in the elimination of the ingress of heated air from the rotor and stator pressure ducts into the stator exhaust ducts [14].

The generator has a closed ventilation cycle. The stator active steel and rotor winding are cooled directly by air, the stator winding is cooled indirectly. The necessary flow rate and circulation of cooling air are provided by two centrifugal fans mounted on the shaft on both sides of the rotor barrel and axial and radial ducts of the rotor winding, the movement through which is carried out due to different radii of rotation at the inlet and outlet of the ducts.

Turbogenerator ventilation block diagram and schematic diagram for cooling the main part of the stator core with loop-shaped cooling ducts are depicted in **Figure 1**.

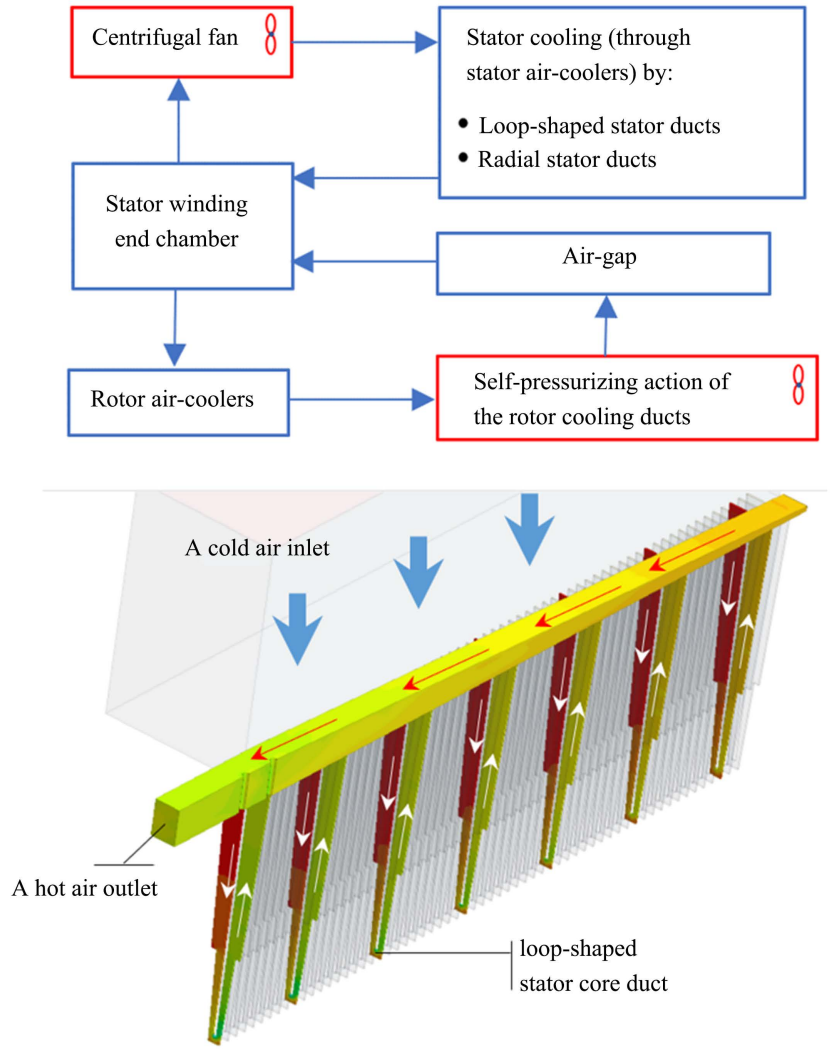

Figure 1. Turbogenerator ventilation block diagram and schematic diagram for cooling the main part of the stator core with loop-shaped cooling ducts.

The present paper considers the algorithm of numerical simulation of the cooling duct of the loop-shaped stator core of the stator of the turbogenerator of the T3FP series of high power. The aim of this study is to examine the nature of airflow in the duct, identify areas of recirculation, and determine the aerodynamic characteristics.

The numerical algorithm under consideration employs two distinct methods of turbulent flow modelling: firstly, stationary RANS methods utilising the SST turbulence model, and secondly, unsteady LES methods employing the DSG model [15].

The calculation methods are then compared with experimental results on a full-scale physical model. The document provides a concise overview of the experimental procedure conducted on the physical model of the duct, accompanied by a comprehensive evaluation of the measuring equipment employed for the aerodynamic characterisation.

It has been demonstrated that the solution to the unsteady problem of air flow in the considered duct reflects the most natural (physical) character of its flow. Furthermore, it allows fluctuations of the flow to be seen and places of its recirculation to be identified visually. In future studies, this approach will facilitate more precise calculation of the associated heat transfer problems, particularly in the most stressed nodes of the generator, such as rotor cooling, end packages of active steel, and others.

2. Experiment on a Physical Model of the Turbogenerator Stator Duct

The experimental setup consists of an air flow source, a 13.85 mm diameter calibrated measuring nozzle with a Prandtl tube installed in it, a receiver with a static pressure sampling point upstream of the cooling duct inlet, and a mock-up of a single cooling duct. The printed mock-up and 3D model that were studied are presented in Figure 2.

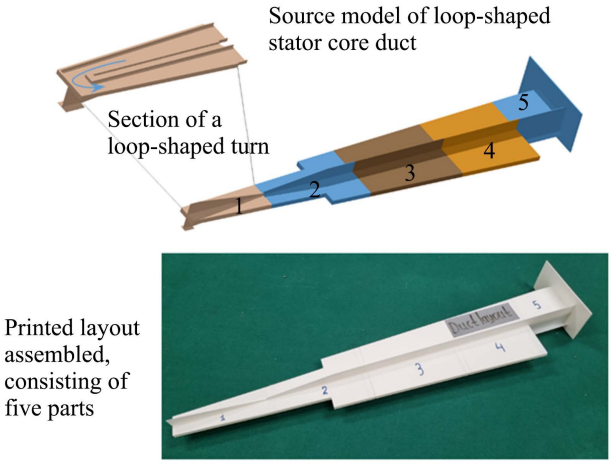

Figure 2. Source model of Loop-shaped duct and printed layout assembly.

The configuration of the object under consideration consists of five constituent parts, which are printed on a 3D printer from PLA plastic. The selection of this number of components is attributable to the geometric constraints of the printer's print area. Each component has been integrated with a spike connection to its counterpart within the mockup, ensuring a robust mechanical linkage is established. The joints are sealed with adhesive. The dimensions of the duct are virtually identical to those of the main stator segment.

2.1. Scope and Methodology of Measurements

The aerodynamic characteristic is dependent upon the pressure drop, which is in turn dependent upon the air flow rate through the duct. In the course of the experiment, the air flow rate was determined by the Prandtl tube in the calibrated measuring nozzle, and the static pressure readings in the receiver were recorded. The schematic diagram of the laboratory model is presented in Figure 3.

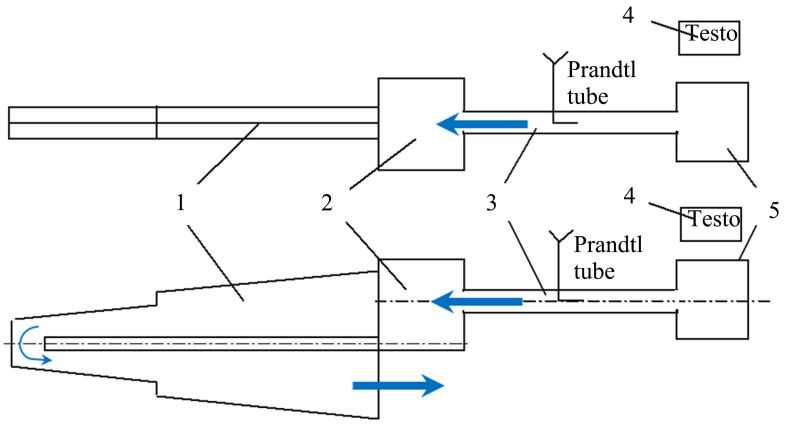

1. Layout of the ventilation duct
2. Receiver
3. Prandtl tube in the calibrated measuring nozzle
4. Differential pressure meter
5. Air flow source

Figure 3. Schematic diagram of the laboratory model.

The mean value obtained from the repetition of the experiment on four occasions (for each Reynolds number) was utilised. The air temperature was measured at 20˚C.

The experimental readings were recorded using the following instruments: the differential pressure meter Testo 512 (20 hPa) and Testo 506 (200 hPa), the Barometer Testo 511, and the Hygrometer Testo 610.

The air flow rate is defined as the product of the average air velocity and the cross-sectional area of the measuring tube. The mean air velocity is determined from the dynamic pressure readings in the measuring tube using the tube coefficients. The air density is determined from the absolute pressure and temperature of the air at the measuring point.

2.2. Measurement Results

The pressure drop for the constructed characteristic is defined as the difference of static pressures at the inlet and outlet of the stator duct. **Figure 4** shows the aerodynamic characteristic of the duct.

The air flow rate of 3.25 l/s shown in **Figure 4** is the design flow rate through one loop-shaped duct and is created by the action of centrifugal fans installed on the rotor. The value of the air flow rate is of paramount importance in ensuring that the thermal margin of the design is maintained at rated load. The design's thermal margin is defined by the limit temperatures of the stator winding and the active steel of the stator core, which are set at 125˚C. It should be noted that this is the expected value of air flow rate through a single loop-shaped duct of the stator core at rated speed of 3000 rpm during operation of the generator. This is specified on the basis of the generator acceptance test data. This value is determined by the calculation department in accordance with the factory methodology.

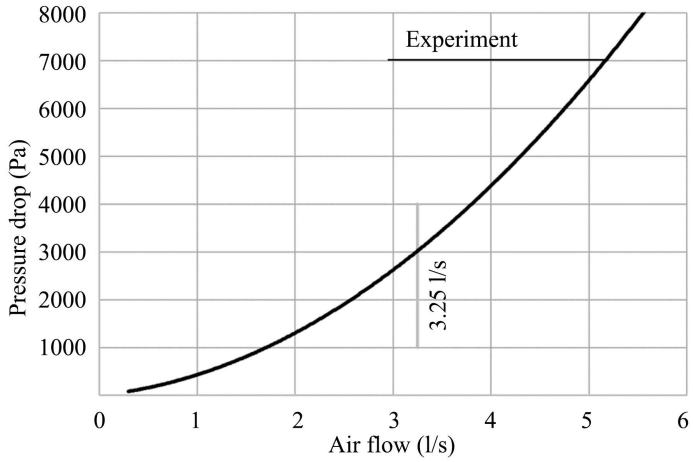

Figure 4. Experimental aerodynamic characterisation of the duct.

3. Numerical Modelling of the Duct

The section presents numerical modelling of a loop-shaped duct. Two methods of turbulent flow modelling are considered in this study: RANS and LES. The most expeditious yet least precise methodologies are the stationary RANS methods. Conversely, RANS do not consider the non-stationarity of the flow, and as such, improvements to the methodology are required. However, RANS steady-state modelling does not require lengthy computation times and can predict the flow with reasonable accuracy. In order to obtain more detailed information on unsteady flow motions, LES methods are utilised. The proposed methodology involves the modelling of small-scale turbulence and the resolution of large-scale turbulence. Concurrently, it necessitates the most extensive grid discretisation and a substantial computational expense.

For each method, a suitable grid discretisation is selected to achieve a specific dimensionless coefficient $y+$. Indeed, this parameter is contingent upon surface roughness. For LES, the grid should be sufficiently fine to resolve small, almost isotropic turbulence scales [16].

Prior to grid construction, an approximate estimation of the initial cell height (Δy) in the prismatic layer configuration was conducted using the Blasius expression, which is based on the determination of local parameters, including the friction coefficient (C_f), wall shear stress (τ_w), and mean velocity (v_{mean}) [17]. A prismatic layer correction was performed for each Reynolds number. In the case of the LES model, the dimensionless coefficient $y+$ was found to be less than 1 in the wall region of the modelled duct. For the SST RANS model, the same parameter was below 5.

Each numerical simulation method is characterised by a common implementation sequence in the form of the following steps: parameterisation of input parameters such as geometries, mesh setup, solver selection and setup, turbulence model specification with appropriate settings, solution and generation of report files. The computational model (see **Figure 5**) consists of a receiver, a duct and the air outlet region of the duct.

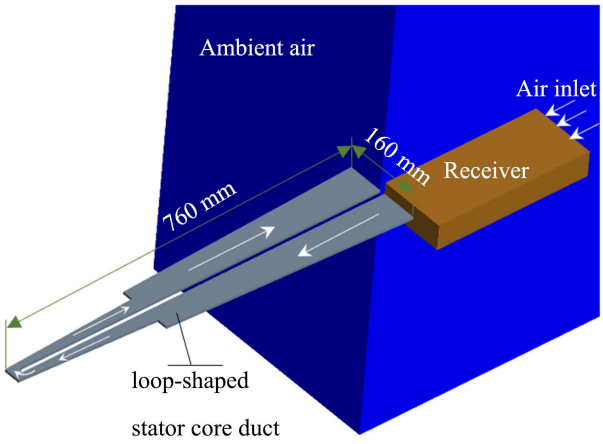

Figure 5. Calculation model.

3.1. RANS Method with SST Turbulent Model

The steady-state and isothermal flow of air is considered in the problem. The air density is assumed constantly and recalculated for the temperature and absolute pressure of the air in the experiment. The Reynolds equations and the finite volume method are utilised for the purpose of modelling.

SST model, a widely employed turbulence model in the field of electrical engineering, has been selected for this study. The model under consideration contains two equations that use the Boussinesq assumption in order to model the Reynolds stress tensor. The Boussinesq assumption is a theoretical framework that establishes a correlation between the Reynolds stress tensor and velocity gradients, thereby facilitating the understanding of turbulent viscosity. This simplification enables the use of a single variable, turbulent viscosity, in lieu of the six unknowns present in the stress tensor [18]. The problem was formulated numerically using the algorithms SIMPLE, AMG Linear Solver, and Gauss-Seidel Relaxation scheme.

The chosen turbulence model combines the advantages of the k-ε and k-ω models for predicting aerodynamic flows and, in particular, for predicting boundary layers at strong unfavourable pressure gradients, which is observed at a sharp turn in the considered duct. To achieve convergence of the solver, the local disbalance of the stored variable in each control volume was below 0.01 (Residual). The value of the dimensionless coefficient *y*+ was selected below 5 by choosing the number of elements in the prismatic layer and specifying the specific height of the layer in the duct region.

The transport equations for the kinetic energy and specific dissipation read (1):

$$\begin{aligned}
&\frac{\partial k}{\partial t}+U_j\frac{\partial k}{\partial x_j}=P_k-\beta^* k\omega+\frac{\partial}{\partial x_j}\left(\left(\nu+\sigma_k\nu_t\right)\frac{\partial k}{\partial x_j}\right),\\
&\frac{\partial \omega}{\partial t}+U_j\frac{\partial \omega}{\partial x_j}=\alpha S^2-\beta\omega^2+\frac{\partial}{\partial x_j}\left(\left(\nu+\sigma_k\nu_t\right)\frac{\partial \omega}{\partial x_j}\right)+2\left(1-F_1\right)\sigma_{\omega 2}\frac{1}{\omega}\frac{\partial k}{\partial x_j}\frac{\partial \omega}{\partial x_j}
\end{aligned} \tag{1}$$

The closure coefficients and equations constants are presented in Table 1.

Table 1. The parameters of SST model.

F_1					
$\tanh\left[\left[\min\left(\max\left(\frac{\sqrt{k}}{\beta^*\omega y},\frac{500\nu}{y^2\omega}\right),\frac{4\rho\sigma_{\omega 2}k}{CD_{k\omega}y^2}\right)\right]^4\right]$					
F_2					
$\tanh\left[\left[\max\left(\frac{2\sqrt{k}}{\beta^*\omega y},\frac{500\nu}{y^2\omega}\right)\right]^2\right]$					
$CD_{k\omega}$			ν_t		P_k
$\max\left(2\rho\sigma_{\omega 2}\frac{1}{\omega}\frac{\partial k}{\partial x_j}\frac{\partial \omega}{\partial x_j},10^{-10}\right)$			$\frac{a_1 k}{\max(a_1\omega, SF_2)}$		$\min\left(\tau_{ij}\frac{\partial U_i}{\partial x_j},10\beta^* k\omega\right)$
Constants					
σ_{k1}	σ_{k2}	$\sigma_{\omega 1}$	$\sigma_{\omega 2}$	γ_1	γ_2
1.176	1.000	2.000	1.168	0.5532	0.4403
β_1	β_2	β^*	κ	a_1	$C_{1\varepsilon}$
0.0750	0.0828	0.0900	0.41	10	10

In the table y is the distance to the nearest wall and ν_t is the turbulent kinematic viscosity. The coefficients of the SST model are a linear combination of the corresponding coefficients of the k-ε and k-ω turbulence models.

3.2. LES Method with the Dynamic Smagorinsky Subgrid Scale Model

The problem under consideration is that of unsteady and isothermal air flow. The air density is assumed constantly and recalculated for the temperature and absolute pressure of the air in the experiment. The modelling process involves the utilisation of subgrid-scale (SGS) models and implicit LES techniques, which are based on the finite volume method. The utilisation of SGS models in conjunction with implicit LES is a methodology that has been employed in this study.

LES balances between accuracy and computational cost, allowing complex turbulent flows to be resolved in greater detail than RANS models, but at a lower cost than full direct numerical simulation (DNS).

In the selection of a mesh for LES turbulence models, a pivotal consideration is the mesh structure and density, which should be adapted to the model's particularities and the physical processes occurring in the flow. The cells should be sufficiently diminutive to capture the substantial vortex structure. It is generally accepted that the diameter of the cell should be smaller than the scale of the vortices that are to be modelled. It is generally recommended that the cell size is set to between 1/20 and 1/50 of the length of the characteristic vortex scale. In the vicin-

ity of walls, it is imperative to employ smaller cells for the purpose of capturing velocity gradients and other pertinent flow parameters. The implementation necessitated the utilisation of a prismatic layer comprising four layers, with a total thickness ranging from 0.1 to 0.2 millimetres, contingent upon the airflow rate through the duct. This corresponded to a y+ value of approximately 1.

The DSG model is utilised, which, in contrast to the classical Smagorinsky model that employs a single constant C_s, calculates a local constant (Germino-Lilly) as a function of flow and time, $C_s = C_s(x, t)$. This approach facilitates the acquisition of the correct resolution of wall-limited flows without the necessity of employing damping functions [19] [20].

Time-Step was chosen 0.005 s with the inner iterations equals 10. Maximum physical time was specified 1.5 s.

3.3. General Assumptions and Boundary Conditions

The boundary conditions adopted in the RANS and LES problem are as follows:

- The entry point to the duct is facilitated by a receiver, the surface of which determines the inlet velocity.
- The exit from the loop-shaped duct is connected to the region on the boundary of which the static pressure condition $P_{st} = 0$ Pa is set.
- In order to enhance the convergence of the problem, the initial velocities were varied in in Cartesian coordinates within the range of {−2, from −3 to −8, 0} m/s.
- The local imbalance of the stored variable in each control volume (residual) was found to be below 0.01.

4. Numerical Simulation Results

The results of the calculation are then subjected to rigorous analysis and validation. The primary arguments have been addressed. The following section will outline the respective advantages and disadvantages of the two methods employed.

4.1. Aerodynamic Characteristics

As illustrated in **Figure 6**, the aerodynamic performance is evaluated through the utilisation of both LES and RANS methodologies, complemented by experimental characterisation.

The characteristics provide close results in the area of the expected design air flow rate of 3.25 l/s (for this purpose, **Figure 5** in the lower right corner shows the calculation deviation from the experimental curve in %). The discrepancy with the experimental value does not exceed 8% for the expected design air flow rate.

4.2. Airflow Distribution

As demonstrated in **Figure 7**, the distribution of the velocity vector within the cross-section of the duct is depicted, along with the distribution at specific moments of time. These moments of time correspond to the solution of the unsteady problem by the LES method, with a calculated air flow of 3.25 l/s.

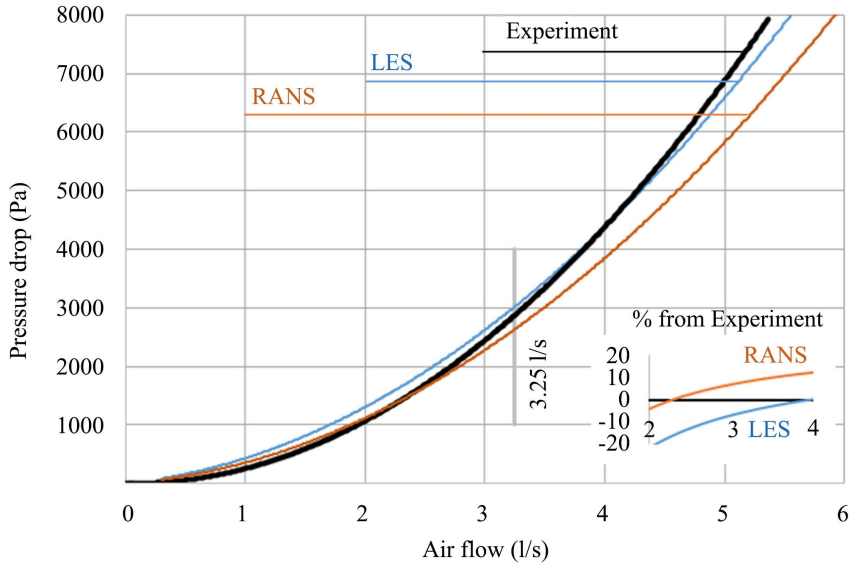

Figure 6. Aerodynamic characteristics by LES and RANS methods.

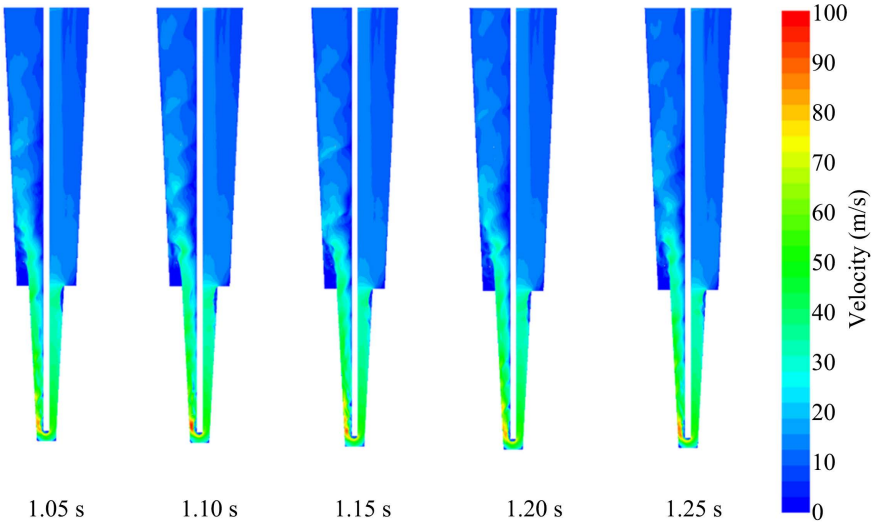

Figure 7. Velocity vector distribution in the duct cross section for an air flow rate of 3.25 l/s.

It is evident that, in accordance with the dynamic flow pattern, vortex formation is manifest in the area of sharp expansion of the cross-section at the point of transition from the tooth to the yoke. It is noteworthy that the intense turbulent flow surrounding the left side of the duct is more pronounced in comparison to the right side, and it is likely that this contributes to a higher degree of heat release, leading to increased losses in that specific region of the duct.

Consequently, the LES method is capable of reflecting the process of air flow in a realistic manner and allows for the estimation of the vortex structure and pressure fluctuations.

As illustrated in Figure 8, the velocity fluctuates at characteristic points over a time period of 0.45 s by LES methos.

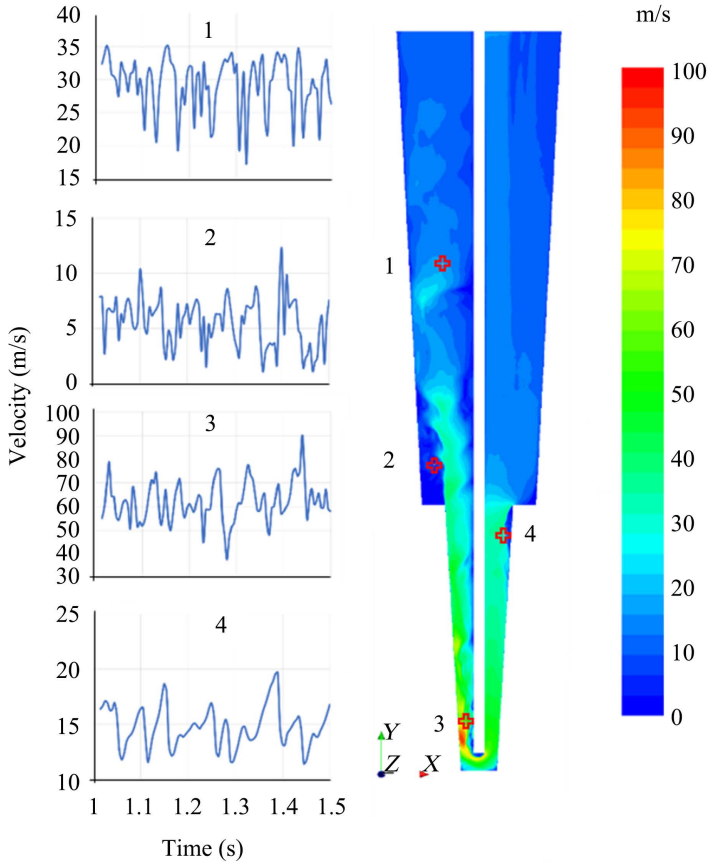

Figure 8. Distribution of velocity vector in the duct cross section for air flow rate 3.25 l/s. over a time. 1, 2, 3, 4-velocity pulsation at characteristic points (red crosses) highlighted by circles.

The steady-state RANS (averaged) air flow pattern is illustrated for the nominal design flow rate (**Figure 9**).

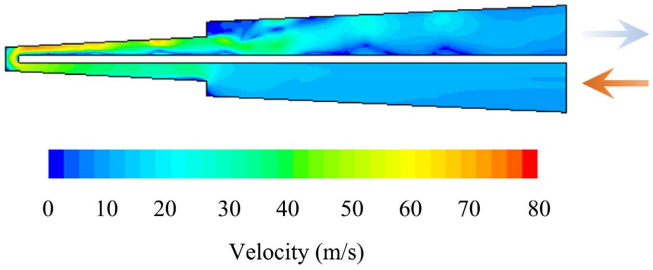

Figure 9. The steady-state air flow pattern is illustrated for a nominal design flow rate of 3.25 l/s.

It is evident that, in general, SST RANS does not necessitate a protracted computation time. It facilitates the acquisition of an averaged depiction of the flow with a satisfactory degree of accuracy. This is achieved without the requirement for labour-intensive tuning of the solver or the duration of the solution itself for the convergence of the problem.

5. Conclusions

The present paper undertakes numerical modelling of the cooling duct of the loop-shaped stator core of an air-cooled turbogenerator stator.

Two methodologies for turbulent flow modelling were considered in order to study the nature of air flow in it, to find the recirculation points and to determine the aerodynamic characteristics. The first methodology was the stationary RANS method using the SST turbulence model. The second methodology was the unsteady LES method using the Smagorinsky dynamic subgrid model.

The validation of the methods was carried out on a full-scale experimental model of the duct. The experimental model was created using additive technologies, specifically, it was produced on a 3D printer from PLA plastic, and it accurately describes the geometry of the duct and the roughness of its surface.

The findings demonstrate that the aerodynamic characteristics derived from the LES and RANS methodologies yield closely aligned results within the anticipated range of the calculated air flow rate of 3.25 l/s at a rated speed 3000 rpm of the turbogenerator. The discrepancy between these calculated values and the experimental measurements is found to be no greater than 8%. Concurrently, the LES method provides a realistic depiction of the temporal progression of airflow, thereby enabling the estimation of vortices and pressure fluctuations. Conversely, RANS does not necessitate a protracted computation time and facilitates the acquisition of an averaged depiction of the flow with a satisfactory degree of accuracy. Moreover, it does not demand labour-intensive tuning of the solver to ensure the convergence of the problem.

Undeniably, the LES method requires further validation on coupled heat transfer problems due to its advantages over RANS, namely the creation of realistic air movement in time, which is especially important when considering heat transfer from the duct walls. It is evident that, in order to enhance the reliability of the calculation results, it is imperative to consider the heat transfer along the gap length, in conjunction with the edge effects of the various cooling schemes of the stator core. This includes radial cooling of the stator edge packets. These considerations should be given due consideration in subsequent studies and in the resolution of coupled heat transfer problems, encompassing the LES and RANS methods, with a view to facilitating a comprehensive comparison. As with any computational method, direct validation is required.

Conflicts of Interest

The authors declare no conflicts of interest regarding the publication of this paper.

References

[1] Žerve, G.K. (1989) Windings of Electric Machines. Energoatomizdat. (In Russian)

[2] Mirabal, L.M., Messal, O., Benabou, A., Le Menach, Y., Chevallier, L., Korecki, J., *et al.* (2022) Iron Loss Modeling of Grain-Oriented Electrical Steels in FEM Simulation Environment. *IEEE Transactions on Magnetics*, **58**, 1-5.

https://doi.org/10.1109/tmag.2021.3097586

[3] Uzhegov, N., Efimov-Soini, N. and Pyrhonen, J. (2016) Assessment of Materials for High-Speed PMSMs Having a Tooth-Coil Topology. *Progress In Electromagnetics Research M*, **51**, 101-111. https://doi.org/10.2528/pierm16080604

[4] Stone, G.C., Culbert, I., Boulter, E.A. and Dhirani, H. (2014) Electrical Insulation for Rotating Machines (Design, Evaluation, Aging, Testing, and Repair). 2nd Edition, Wiley-IEEE Press.

[5] Antoniuk, O.V., Kartashova, T.N. and Roitgarz, M.B. (2013) Increase of Unit Power of Turbogenerators Using New Materials and Technologies. *Novoye v Rossiyskoy elektroenergetika*, No. 5, 5-17. (In Russian)

[6] Joho, R., Picech, C. and Mayor, K. (2006) Large Air-Cooled Turbogenerators—Extending the Boundaries. Alstom, CIGRE 2006, Paper A1-106.

[7] Khutoretsky, G.M., Gurevich, E.I. and Petrov, A.G. (1983) Experience of Cooling Intensification of the 500 MW Turbogenerators at NPP. *Electrical Power Plants*, No. 11, 9-16. (In Russian)

[8] Zhou, G., Han, L., Fan, Z., Zhang, H., Dong, X., Wang, J., *et al.* (2018) Ventilation Cooling Design for a Novel 350-MW Air-Cooled Turbo Generator. *IEEE Access*, **6**, 62184-62192. https://doi.org/10.1109/access.2018.2875757

[9] GE VERNOVA, Air-Cooled Generator, Specifications. https://www.gevernova.com/gas-power/products/generators/air-cooled

[10] Sienens Energy, SGen-100A and SGen-1000A, Specifications. https://www.siemens-energy.com/global/en/home/products-services/product/sgen-100a.html#SGen-1000A

[11] Zhang, S., Wang, F., Zhang, Y., Gao, W. and Xiang, C. (2024) A Comparative Study on Coupled Fluid-Thermal Field of a Large Nuclear Turbine Generator with Radial and Composited Radial-Axial-Radial Ventilation Systems. *Machines*, **12**, Article No. 326. https://doi.org/10.3390/machines12050326

[12] Korovkin, N.V., Verkhovtsev, D. and Gulay, S. (2021) Rotor Air-Cooling Efficiency of Powerful Turbogenerator. *IEEE Transactions on Energy Conversion*, **36**, 1983-1990. https://doi.org/10.1109/tec.2020.3045063

[13] Verkhovtsev, D.A., Maiantcev, M.A. and Permut, A.S. (2025) Optimisation of Air-Cooled Turbogenerator Rotor Sub-Slot Duct Shape by NSGA-II. *Scientific Research of the SCO Countries*: *Synergy and Integration*, *Part* 2, Beijing, 2 July 2025, 156-163. https://doi.org/10.34660/inf.2025.43.71.030

[14] Antonjuk, O., Kartashova, T. and Roytgarts, M. (2009) Series of Air-Cooled Turbogenerators of Power up to 410 MVA. *International Conference POWER-GEN Europe*, Cologne, 26-28 May 2009.

[15] ANSYS FLUENT 12.0 Theory Guide.

[16] Nichols, R.H. (2010) Turbulence Models and Their Application to Complex Flows. University of Alabama at Birmingham, Revision 4.01. https://www.researchgate.net/publication/281117306_Turbulence_Models_and_Their_Application_to_Complex_Flows

[17] Durst, F., Kikura, H., Lekakis, I., Jovanović, J. and Ye, Q. (1996) Wall Shear Stress Determination from Near-Wall Mean Velocity Data in Turbulent Pipe and Channel Flows. *Experiments in Fluids*, **20**, 417-428. https://doi.org/10.1007/bf00189380

[18] Lien, F.S. and Leschziner, M.A. (1993) Computational Modelling of 3D Turbulent Flow in S-Diffuser and Transition Ducts. *Proceedings of the* 2*nd International Symposium on Engineering Turbulence Modelling and Measurements*, Florence, 31 May

-2 June 1993, 217-228. https://doi.org/10.1016/b978-0-444-89802-9.50025-3

[19] Germano, M., Piomelli, U., Moin, P. and Cabot, W.H. (1991) A Dynamic Subgrid-Scale Eddy Viscosity Model. *Physics of Fluids A*: *Fluid Dynamics*, **3**, 1760-1765. https://doi.org/10.1063/1.857955

[20] Lilly, D.K. (1992) A Proposed Modification of the Germano Subgrid-Scale Closure Method. *Physics of Fluids A*: *Fluid Dynamics*, **4**, 633-635. https://doi.org/10.1063/1.858280